COMMUNICATION

A Green Route to Conjugated Polyelectrolyte Interlayers for High Performance Solar Cells

Jegadesan Subbiah, Valerie D. Mitchell, Nicholas K. C. Hui, David J. Jones* and Wallace W. H. Wong*[a]

Abstract: Synthesis of fluorene-based conjugated polyelectrolytes was achieved via Suzuki polycondensation in water and completely open to air. The polyelectrolytes were conveniently purified by dialysis and analysis of the materials showed properties expected for fluorene-based conjugated polyelectrolytes. The materials were then employed in solar cell devices as an interlayer in conjunction with ZnO. The double interlayer led to enhanced power conversion efficiency of 10.75% and 15.1% for polymer and perovskite solar cells respectively.

Organic photovoltaics are considered a promising solar energy conversion technology due to their potential to provide large area solution-processable, lightweight, low-cost and flexible devices.[1] Over the past few years, power conversion efficiencies (PCEs) of over 11% have been achieved for polymer-based single-junction organic photovoltaic (OPV) devices with bulk heterojunction (BHJ) architectures.[2] This progress can be attributed to improvements in device architecture, device processing, engineering of the interface between electrode and active layer, and the development of new electron-donor and electron-acceptor materials.[3, 4]

Most of the high-efficiency OPV devices employ inverted device geometries because metal oxide interlayers such as zinc oxide (ZnO), titanium oxide (TiO_x), tin oxide (SnO_x), nickel oxide (NiO), and molybdenum oxide (MoO_x), provide enhanced stability as well as device performance.[5, 6] Among the various metal oxides, zinc oxide (ZnO) is a promising electron transport layer (ETL) because of its stability, transparency, facile synthesis and high mobility.[7] However, the intrinsic surface defects and the poor contact at the inorganic/organic interface of the metal oxide ETL and BHJ photoactive layer limit the charge extraction and transport efficiencies. This decreases the charge carrier collection efficiency at the electrode, resulting in a poor short-circuit current density (J_{sc}) and a low fill factor (FF).[8]

To circumvent these issues, ultra-thin buffer layers comprised of self-assembled monolayers, ionic liquid molecules, and fullerene derivatives have been introduced to modify the ZnO ETL.[9] The ultrathin buffer layer provides improved adhesion between the metal oxide interlayer and BHJ active layer, enhanced electron transfer from active layer to electrode, and increased built-in potential due to the dipolar nature of the interlayer.[10] Recently, an ultra-thin layer of a fullerene derivative (PCBE-OH) deposited on a ZnO layer was employed as the cathode buffer layer for inverted OPV in conjunction with the high performance donor polymer PBDT-BT to give a maximum PCE of 9.4%.[11, 12] Here, the PCBE-OH buffer layer enhances the electron collection efficiency of the inverted devices by smoothening and passivating the ZnO surface. Alternatively, the use of conjugated polyelectrolytes (CPEs), which feature a delocalized π−π conjugated backbone with pendant ionic groups, has emerged as a promising design for the cathode interface modifier.[13] The CPE buffer layer improves device efficiency by facilitating charge transport and collection through the formation of permanent dipole moments at the metal organic interfaces.[14] In earlier reports, a polyfluorene-based CPE, commonly known as PFN, has been used both as a single[4] and double[15] interlayer material with ZnO giving enhanced performance in polymer-fullerene active layer devices. In addition to BHJ OPV devices, it is also important to develop appropriate interlayer materials for more stable and efficient perovskite solar cells.[16]

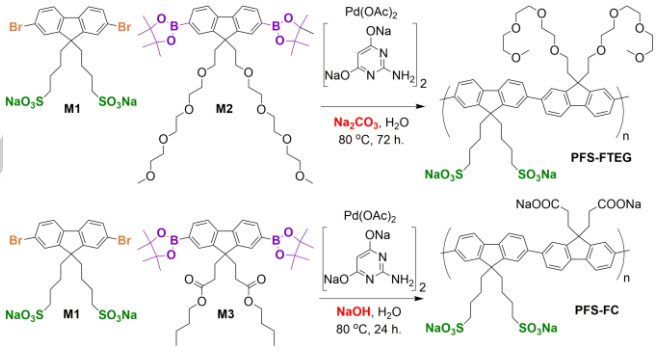

Figure 1. Synthesis of conjugated polyelectrolyte (CPE) materials **PFS-FTEG** and **PFS-FC** via Suzuki polycondensation in water and air.

In this study, we synthesized two polyfluorene-based CPEs (**PFS-FTEG** and **PFS-FC**) using an innovative aqueous Suzuki polycondensation approach (Figure 1). The most common synthetic method for generating CPEs proceeds through a polymerization of neutral precursor monomers followed by post-polymerization modification to install the ionic functionalities.[17, 18] The precursor route allows the use of common polymerization catalyst systems to generate an easily analyzed neutral polymer intermediate.[17] However, this approach suffers from several drawbacks. The post-polymerization modification must proceed at extremely high conversion rates to generate the electronically homogenous material required for reproducibility in OPV applications. This requirement for high conversion rates is further complicated by the fact that as the reaction proceeds and a

[a] Dr J. Subbiah, V. D. Mitchell, N. K. C. Hui, Dr D. J. Jones, Dr. W. W. H. Wong
School of Chemistry
The University of Melbourne
Bio21 Institute, 30 Flemington Road, Parkville, Victoria 3010, Australia
E-mail: djjones@unimelb.edu.au; wwhwong@unimelb.edu.au

Supporting information for this article is given via a link at the end of the document.

nonpolar moiety is made ionic, the solubility of the substrate in the reaction mixture changes dramatically. Finally and perhaps most importantly, the conventional polymerizations used in the precursor route (eg. Stille, Suzuki, Sonagashira, Negishi, or Yamamoto couplings)[19] often employ hazardous organic solvents and/or energy-intensive reaction conditions.

The ideal synthesis for industrial applications would employ green solvents (water or alcohols) under ambient atmosphere. For this reason, we decided to investigate CPE preparation using an aqueous Suzuki coupling method initially developed for bioconjugation.[20] The adoption of this synthetic procedure, which employs pyrimidine ligands rather than oxidatively unstable phosphine ligands, allows synthesis of the target CPEs in water with no organic co-solvents and completely open to air. Moreover, the choice of aqueous solvent facilitates polymerization of the ionic monomers directly. Monomer building block **M1** with charged sulfonate groups was synthesized and coupled either with tetraethylene glycol-substituted fluorene boronic acid ester **M2** or carboxylate precursor **M3** (Figure 1) to generate the CPEs **PFS-FTEG** and **PFS-FC** respectively. The crude CPE products were then simply purified by dialysis (see Supporting Information for full synthetic details and characterization). Gel permeation chromatography of polyelectrolytes can be complicated and require specialty equipment, often leading researchers to resort to rough estimates of molecular weights of polymer products.[21] As the CPEs in this study were susceptible to acidification, addition of HCl generated the corresponding polyacids, greatly facilitating GPC analysis. The acidified CPE samples showed number average molecular weights of 10.6 and 93 kg/mol for **PFS-FTEG** and **PFS-FC** respectively. The UV-Vis absorption profiles and frontier orbital energies of these CPEs are comparable to other polyfluorene-based CPEs in the literature (see Supporting Information for data).[18, 22]

The CPE materials generated were then used in the fabrication of inverted OPV devices with a ZnO/CPE bilayer as the ETL. The molecular structure of the photoactive layer materials PTB7-Th and $PC_{71}BM$ as well as the energy levels of the components used in the devices are shown in Figure 2a and 2b, respectively. The CPE layers were deposited by spin coating from ethanol giving layer thicknesses of ~5 nm. Films of ZnO, ZnO/**PFS-FTEG** and ZnO/**PFS-FC** deposited on ITO substrates possessed high transparency with >80% average transmittance in the visible region (Figure 2c).

To investigate the effect of CPE materials on the ZnO layer, photoluminescence (PL) measurements of ZnO, ZnO/**PFS-FTEG** and ZnO/**PFS-FC** films on ITO coated glass substrate were recorded (Figure 2d). For the ZnO coated substrate a strong broad emission band at 540 nm was observed, indicating the presence of defect states in ZnO.[23] Upon deposition of either **PFS-FTEG** or **PFS-FC** layer on the ZnO film, the PL emission at 540 nm was quenched completely thus confirming the formation of a CPE layer on the ZnO surface as well as passivation of defect state (oxygen vacancy) in ZnO layer. Here, the ultra-thin CPE layer coordinate with ZnO by sharing lone electron pair of oxygen in the polar side-chain group of the conjugated polyelectrolyte, which effectively passivate the defect state of ZnO.[24] Similar effect of surface passivation was reported earlier by our group using self-assembled PCBE-OH layer on ZnO surface for passivation of defect state.[11] In addition to surface passivation, the CPE layer can also improve charge transport at the interface. Atomic force microscopy (AFM) showed reduced roughness of the ZnO surface on treatment with the CPE solutions (Supporting information Figure S8 & S9). Scanning Kelvin probe microscopy experiments revealed higher surface energy values for CPE treated films (Figure S10). Both the improved surface smoothness and surface energy should have a positive impact on interfacial contact and, ultimately, performance in devices.

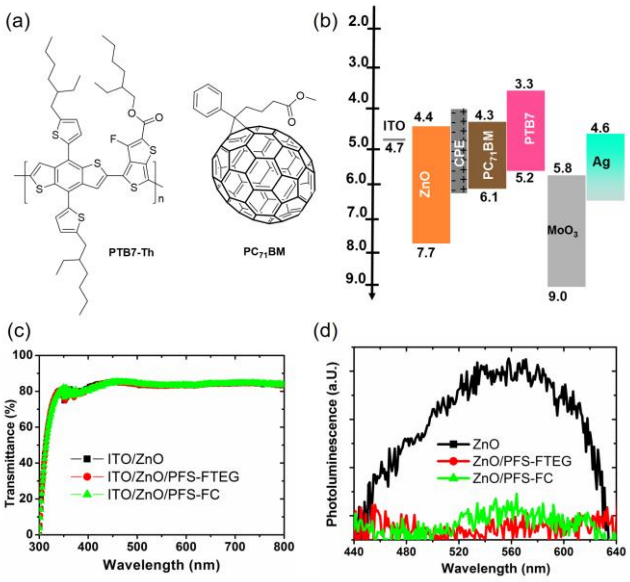

Figure 2. a) Molecular structure of PTB7-Th and $PC_{71}BM$; (b) Energy level diagram of the components used in OPV device; (c) Optical transmittance spectra and (d) Photoluminescence spectra for ITO/ZnO, ITO/ZnO/**PFS-FTEG** and ITO/ZnO/**PFS-FC** film.

Inverted OPV devices were fabricated with the architecture shown in Figure 3a. Table 1 summarizes the performance characteristics of solar cell devices including open-circuit voltage (V_{oc}), short-circuit current density (J_{sc}) and fill factor (*FF*), under 1 sun illumination. The current density−voltage (*J*−*V*) characteristics of these OPV devices are shown in Figure 3b. The inverted OPV device with ZnO-only ETL showed a very good PCE of 9.7% in line with literature reports.[12] The use of either **PFS-FTEG** or **PFS-FC** CPEs improved the device performance to 10.75% and 10.3% respectively. The enhanced PCE was mainly due to the significant increase in J_{sc} and *FF*. We also fabricated devices with CPE layer alone and the *J*-*V* curve is shown in Figure S7. The devices with pure CPE layer had significantly lower power conversion efficiency compared to ZnO/CPE devices (Table S2). The CPE only devices all showed low fill factors and this could be a result of poor surface coverage of the CPE material on ITO. Good surface coverage of interlayer materials is essential for high performance.[25]

The external quantum efficiency (EQE) spectrum (Figure 3c) of the devices confirmed current enhancement across the entire absorption range. By integrating the EQE spectra, the calculated J_{sc} of 16.8, 17.60 and 17.40 mA/cm^2 were obtained for the ZnO, ZnO/**PFS-FTEG** and ZnO/**PFS-FC** devices respectively which were in good agreement with *J*-*V* measurements as shown in Table 1. In more detailed current-voltage experiments (see Supporting Information for data and discussion, Figure S11), there was strong evidence that the improved J_{sc} with CPE devices

was the result of improved charge extraction at the active layer/ETL interface and charge collection at the electrodes.[26] Improved diode characteristics were also observed for CPE devices in dark current experiments indicating efficient electron collection at the cathode interface enabled by the high-lying lowest unoccupied molecular orbital (LUMO) energy levels of the buffer layers (Figure S12).[27] Lower resistance was measured for devices containing CPE buffer layers in alternating current (AC) impedance spectroscopy experiments further supporting the current-voltage device performance results (Figure 3d).

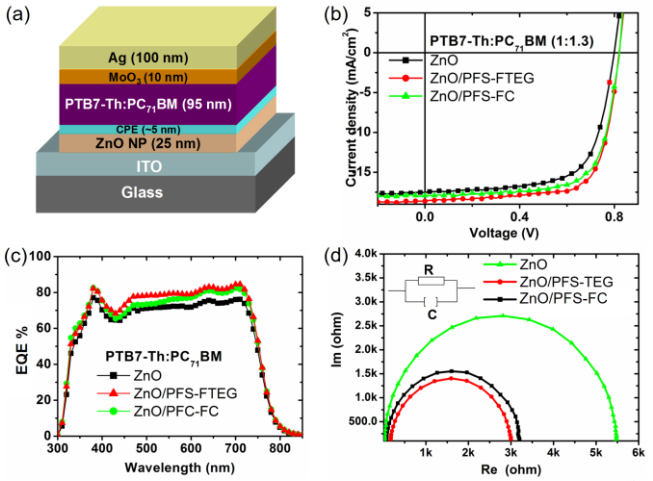

Figure 3. (a) Schematic diagram of inverted device geometry and (b) J-V curve; (c) EQE spectrum and; (d) Nyquist plot (electrical impedance) of the BHJ solar cells containing various ETLs ZnO, ZnO/**PFS-FTEG** and ZnO/**PFS-FC**.

Table 1. Photovoltaic performance of PTB7-Th:$PC_{71}BM$ solar cells.[a]

Interlayers	J_{sc} (mA/cm^2)	V_{oc} (V)	*FF* (%)	PCE (%)
ZnO	17.5 ±0.25	0.78 ±0.01	67 ±2	9.50 ± 0.20 (9.7)
ZnO/**PFS-FTEG**	18.3 ±0.20	0.80 ±0.02	72 ±2	10.60 ± 0.15 (10.75)
ZnO/**PFS-FC**	18.0 ±0.30	0.80 ±0.02	69 ±3	10.10 ± 0.20 (10.30)

[a] Average values and standard deviation of device statistics from 10 devices are given in parentheses

The CPE interlayer materials were also deployed in perovskite solar cell devices. The device geometry of the perovskite devices is shown in Figure 4a.[5, 28] Detailed device fabrication conditions are provided in the Supporting Information. The *J*–*V* characteristics of planar methylammonium lead iodide ($MAPbI_3$)-based perovskite solar cells with ZnO, ZnO/**PFS-FTEG** and ZnO/**PFS-FC** as ETL are shown in Figure 4b and their photovoltaic properties are summarized in Table 2. The device with ZnO-only ETL gave an average PCE of 12.0% with significant enhancements observed for devices using the CPE interlayers. Maximum PCE of 15.1% was obtained for the ZnO/**PFS-FTEG** device. As in the BHJ OPVs, the increase in the J_{sc} observed in devices with the CPE buffer layer suggested that the CPE layer forms a better interface with the perovskite film leading to improved electron extraction through suppression of non-geminate recombination.[29] To illustrate device reproducibility, a histogram of device performance obtained from 20 devices is provided in Figure S13. Greater than 70% of the devices gave PCEs over 15% with a standard deviation of 0.3%.

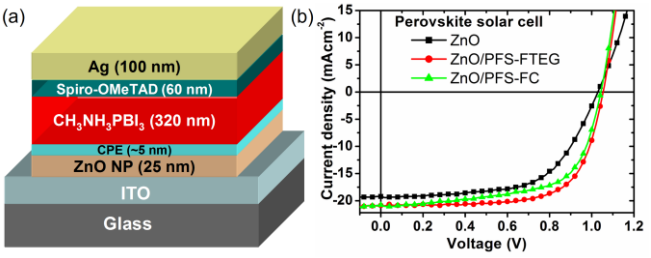

Figure 4. (a) Schematic diagram of perovskite solar cell and (b) J-V curves of the perovskite devices with various electron transport layers ZnO, ZnO/**PFS-FTEG** and ZnO/**PFS-FC**.

Table 2. Statistics and best photovoltaic parameter for perovskite solar cells with various ETLs.[a]

Interlayers	J_{sc} (mA/cm^2)	V_{oc} (V)	*FF* (%)	PCE (%)
ZnO	19.2 ±0.20	1.02 ±0.02	61 ±3	11.75 ± 0.25 (12.0)
ZnO/**PFS-FTEG**	20.9 ±0.25	1.04 ±0.01	69 ±2	14.90 ± 0.20 (15.1)
ZnO/**PFS-FC**	20.8 ±0.35	1.04 ±0.02	64 ±3	13.60 ± 0.30 (13.9)

[a] Average values and standard deviation of device statistics from 10 devices are given in parentheses

In summary, inverted OPV and perovskite devices with maximum PCEs of 10.75% and 15.1% respectively were fabricated through incorporation of a solution processed ZnO/**PFS-FTEG** interlayer. Two novel CPE interlayer materials, **PFS-FTEG** and **PFS-FC**, were synthesized via Suzuki polycondensation in water without organic co-solvents in air. These fluorene-based CPE materials produced interlayers that exhibited high transparency and smooth surface morpholgy while lowering the work function of ZnO coated ITO substrates. With this double interlayer, enhanced photovoltaic properties were observed compared to ZnO-only devices. The high performance of OPV and perovskite devices resulted from the use of an ultrathin CPE buffer layer which improved the charge collection efficiency by suppressing non-geminate recombination and decreasing series resistance. These results showed that the CPE modified ZnO ETL is an attractive way to improve performance of OPV and perovskite devices especially for large-area fully printed applications.

Experimental Section

Detailed synthesis procedures and characterisation data for the CPE materials as well as device fabrication procedures and characterisation can be found in the Supporting Information.

Acknowledgements

This work was made possible by support from the Australian Renewable Energy Agency which funds the project grants within the Australian Centre for Advanced Photovoltaics (ACAP). Responsibility for the views, information or advice expressed herein is not accepted by the Australian Government. WWHW is supported by an ARC Future Fellowship (FT130100500). We thank CSIRO for access to the device measurements and glove box equipment. This work was performed in part at the Melbourne Centre for Nanofabrication (MCN) in the Victorian Node of the Australian National Fabrication Facility (ANFF). This work was also performed in part at the Materials Characterisation and Fabrication Platform (MCFP) at the University of Melbourne.

Keywords: conjugated polyelectrolyte • Suzuki polycondensation • interlayer material • polymer solar cell • perovskite solar cell

[1] G. Li, R. Zhu, Y. Yang, *Nat. Photon.* **2012**, *6*, 153-161.

[2] L. Nian, K. Gao, F. Liu, Y. Kan, X. Jiang, L. Liu, Z. Xie, X. Peng, T. P. Russell, Y. Ma, *Adv. Mater.* **2016**, *28*, 8184-8190.

[3] Y. Lin, F. Zhao, Q. He, L. Huo, Y. Wu, T. C. Parker, W. Ma, Y. Sun, C. Wang, D. Zhu, A. J. Heeger, S. R. Marder, X. Zhan, *J. Am. Chem. Soc.* **2016**, *138*, 4955-4961; Z. He, B. Xiao, F. Liu, H. Wu, Y. Yang, S. Xiao, C. Wang, T. P. Russell, Y. Cao, *Nat. Photon.* **2015**, *9*, 174-179; C. E. Small, S. Chen, J. Subbiah, C. M. Amb, S.-W. Tsang, T.-H. Lai, J. R. Reynolds, F. So, *Nat. Photon.* **2012**, *6*, 115-120; M. Grätzel, R. A. J. Janssen, D. B. Mitzi, E. H. Sargent, *Nature* **2012**, *488*, 304-312.

[4] Z. He, C. Zhong, S. Su, M. Xu, H. Wu, Y. Cao, *Nat. Photon.* **2012**, *6*, 593-597.

[5] J. You, L. Meng, T.-B. Song, T.-F. Guo, Y. Yang, W.-H. Chang, Z. Hong, H. Chen, H. Zhou, Q. Chen, Y. Liu, N. De Marco, Y. Yang, *Nat. Nanotechnol.* **2016**, *11*, 75-81.

[6] S.-H. Liao, H.-J. Jhuo, P.-N. Yeh, Y.-S. Cheng, Y.-L. Li, Y.-H. Lee, S. Sharma, S.-A. Chen, *Sci. Rep.* **2014**, *4*, 6813; J. R. Manders, S.-W. Tsang, M. J. Hartel, T.-H. Lai, S. Chen, C. M. Amb, J. R. Reynolds, F. So, *Adv. Funct. Mater.* **2013**, *23*, 2993-3001; C.-C. Chueh, C.-Z. Li, A. K. Y. Jen, *Energy Environ. Sci.* **2015**, *8*, 1160-1189.

[7] Z. Liang, Q. Zhang, O. Wiranwetchayan, J. Xi, Z. Yang, K. Park, C. Li, G. Cao, *Adv. Funct. Mater.* **2012**, *22*, 2194-2201; Y. Sun, J. H. Seo, C. J. Takacs, J. Seifter, A. J. Heeger, *Adv. Mater.* **2011**, *23*, 1679-1683.

[8] H. Ma, H.-L. Yip, F. Huang, A. K. Y. Jen, *Adv. Funct. Mater.* **2010**, *20*, 1371-1388; C. Liu, Y. Tan, C. Li, F. Wu, L. Chen, Y. Chen, *ACS Appl. Mater. Interfaces* **2015**, *7*, 19024-19033.

[9] Y.-J. Cheng, C.-H. Hsieh, Y. He, C.-S. Hsu, Y. Li, *J. Am. Chem. Soc.* **2010**, *132*, 17381-17383; B. R. Lee, H. Choi, J. SunPark, H. J. Lee, S. O. Kim, J. Y. Kim, M. H. Song, *J. Mater. Chem.* **2011**, *21*, 2051-2053; I. Lange, S. Reiter, J. Kniepert, F. Piersimoni, M. Pätzel, J. Hildebrandt, T. Brenner, S. Hecht, D. Neher, *Appl. Phys. Lett.* **2015**, *106*, 113302; S. Nam, J. Seo, S. Woo, W. H. Kim, H. Kim, D. D. C. Bradley, Y. Kim, *Nat. Commun.* **2015**, *6*, 8929.

[10] Y. Zhong, J. Ma, K. Hashimoto, K. Tajima, *Adv. Mater.* **2013**, *25*, 1071-1075.

[11] J. Subbiah, B. Purushothaman, M. Chen, T. Qin, M. Gao, D. Vak, F. H. Scholes, X. Chen, S. E. Watkins, G. J. Wilson, A. B. Holmes, W. W. H. Wong, D. J. Jones, *Adv. Mater.* **2014**, *27*, 702-705.

[12] S.-H. Liao, H.-J. Jhuo, Y.-S. Cheng, S.-A. Chen, *Adv. Mater.* **2013**, *25*, 4766-4771.

[13] C. V. Hoven, A. Garcia, G. C. Bazan, T.-Q. Nguyen, *Adv. Mater.* **2008**, *20*, 3793-3810; H. Choi, C.-K. Mai, H.-B. Kim, J. Jeong, S. Song, G. C. Bazan, J. Y. Kim, A. J. Heeger, *Nat. Commun.* **2015**, *6*, 7348; C. Duan, K. Zhang, X. Guan, C. Zhong, H. Xie, F. Huang, J. Chen, J. Peng, Y. Cao, *Chem. Sci.* **2013**, *4*, 1298-1307; Y. Liu, Z. A. Page, T. P. Russell, T. Emrick, *Angew. Chem. Int. Ed.* **2015**, *54*, 11485-11489; Z. Hu, K. Zhang, F. Huang, Y. Cao, *Chem. Commun.* **2015**, *51*, 5572-5585; C. Duan, K. Zhang, C. Zhong, F. Huang, Y. Cao, *Chem. Soc. Rev.* **2013**, *42*, 9071-9104.

[14] Y.-M. Chang, C.-Y. Leu, *J. Mater. Chem. A* **2013**, *1*, 6446-6451; R. Xia, D.-S. Leem, T. Kirchartz, S. Spencer, C. Murphy, Z. He, H. Wu, S. Su, Y. Cao, J. S. Kim, J. C. deMello, D. D. C. Bradley, J. Nelson, *Adv. Energy Mater.* **2013**, *3*, 718-723.

[15] T. Yang, M. Wang, C. Duan, X. Hu, L. Huang, J. Peng, F. Huang, X. Gong, *Energy Environ. Sci.* **2012**, *5*, 8208-8214.

[16] S. S. Reddy, K. Gunasekar, J. H. Heo, S. H. Im, C. S. Kim, D.-H. Kim, J. H. Moon, J. Y. Lee, M. Song, S.-H. Jin, *Adv. Mater.* **2016**, *28*, 686-693.

[17] H. Jiang, P. Taranekar, J. R. Reynolds, K. S. Schanze, *Angew. Chem. Int. Ed.* **2009**, *48*, 4300-4316.

[18] W. Lee, J. H. Seo, H. Y. Woo, *Polymer* **2013**, *54*, 5104-5121.

[19] G. C. Bazan, Z. Henson, in *Encyclopedia of Polymeric Nanomaterials* (Eds.: S. Kobayashi, K. Müllen), Springer Berlin Heidelberg, Berlin, Heidelberg, **2015**, pp. 427-433.

[20] J. M. Chalker, C. S. C. Wood, B. G. Davis, *J. Am. Chem. Soc.* **2009**, *131*, 16346-16347.

[21] C. Tan, M. R. Pinto, K. S. Schanze, *Chem. Commun.* **2002**, 446-447.

[22] F. Huang, H. Wu, D. Wang, W. Yang, Y. Cao, *Chem. Mater.* **2004**, *16*, 708-716.

[23] V. Ischenko, S. Polarz, D. Grote, V. Stavarache, K. Fink, M. Driess, *Adv. Funct. Mater.* **2005**, *15*, 1945-1954.

[24] S. Shao, K. Zheng, T. Pullerits, F. Zhang, *ACS Appl. Mater. Interfaces* **2013**, *5*, 380-385.

[25] K. Zhang, Z. Hu, R. Xu, X.-F. Jiang, H.-L. Yip, F. Huang, Y. Cao, *Adv. Mater.* **2015**, *27*, 3607-3613; R. Kang, S.-H. Oh, D.-Y. Kim, *ACS Appl. Mater. Interfaces* **2014**, *6*, 6227-6236.

[26] J. Kniepert, I. Lange, J. Heidbrink, J. Kurpiers, T. J. K. Brenner, L. J. A. Koster, D. Neher, *J. Phys. Chem. C* **2015**, *119*, 8310-8320.

[27] C.-Z. Li, C.-Y. Chang, Y. Zang, H.-X. Ju, C.-C. Chueh, P.-W. Liang, N. Cho, D. S. Ginger, A. K. Y. Jen, *Adv. Mater.* **2014**, *26*, 6262-6267.

[28] D. Liu, T. L. Kelly, *Nat. Photon.* **2014**, *8*, 133-138; J. H. Heo, D. H. Song, H. J. Han, S. Y. Kim, J. H. Kim, D. Kim, H. W. Shin, T. K. Ahn, C. Wolf, T.-W. Lee, S. H. Im, *Adv. Mater.* **2015**, *27*, 3424-3430.

[29] C. Sun, Z. Wu, H.-L. Yip, H. Zhang, X.-F. Jiang, Q. Xue, Z. Hu, Z. Hu, Y. Shen, M. Wang, F. Huang, Y. Cao, *Adv. Energy Mater.* **2015**, *6*, 1501534; M. Saliba, S. Orlandi, T. Matsui, S. Aghazada, M. Cavazzini, J.-P. Correa-Baena, P. Gao, R. Scopelliti, E. Mosconi, K.-H. Dahmen, *Nat. Energy* **2016**, *1*, 15017.

Entry for the Table of Contents

COMMUNICATION

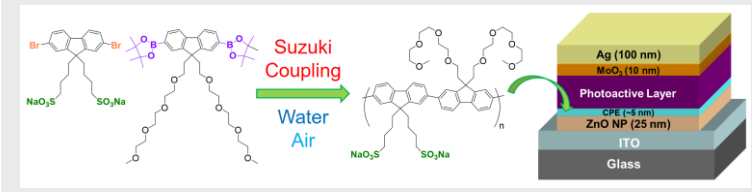

Fluorene-based conjugated polyelectrolytes were prepared using a green synthetic route with polymerization in water and in air. High performance polymer and perovskite solar cells were fabricated using the polyelectrolytes in the cathode interlayer giving power conversion efficiency of 10.75% and 15.1%.

Jegadesan Subbiah, Valerie D. Mitchell, Nicholas K. C. Hui, David J. Jones and Wallace W. H. Wong**

Page No. – Page No.

A Green Route to Conjugated Polyelectrolyte Interlayers for High Performance Solar Cells

Author/s:
Subbiah, J; Mitchell, VD; Hui, NKC; Jones, DJ; Wong, WWH

Title:
A Green Route to Conjugated Polyelectrolyte Interlayers for High-Performance Solar Cells

Date:
2017-07-10

Citation:
Subbiah, J., Mitchell, V. D., Hui, N. K. C., Jones, D. J. & Wong, W. W. H. (2017). A Green Route to Conjugated Polyelectrolyte Interlayers for High-Performance Solar Cells. Angewandte Chemie International Edition, 56 (29), pp.8431-8434. https://doi.org/10.1002/anie.201612021.